Spectroscopic and Biochemical Characterization of Heme Binding to Yeast Dap1p and Mouse PGRMC1p†

Kaushik Ghosh,‡,§ Alisha M. Thompson,‡,§ Robert A. Goldbeck,‡ Xiaoli Shi,⊥ Stephanie Whitman,‡ Eric Oh,∥ Zhu Zhiwu,⊥ Chris Vulpe,∥ and Theodore R. Holman*,‡

Department of Chemistry and Biochemistry, University of California, Santa Cruz, California 95064, Department of Environmental Toxicology, University of California, Santa Cruz, California 95064, and Department of Nutritional Sciences and Toxicology, University of California, Berkeley, California 94044

Received June 15, 2005; Revised Manuscript Received September 26, 2005

ABSTRACT: Yeast damage-associated response protein (Dap1p) and mouse progesterone receptor membrane component-1 protein (mPGRMC1p) belong to a highly conserved class of putative membrane-associated progesterone binding proteins (MAPR), with Dap1p and inner zone antigen (IZA), the rat homologue of mPGRMC1p, recently being reported to bind heme. While primary structure analysis reveals similarities to the cytochrome b_5 motif, neither of the two axial histidines responsible for ligation to the heme is present in any of the MAPR proteins. In this paper, EPR, MCD, CD, UV−vis, and general biochemical methods have been used to characterize the nature of heme binding in both Dap1p and a His-tagged, membrane anchor-truncated mPGRMC1p. As isolated, Dap1p is a tetramer which can be converted to a dimer upon addition of 150 mM salt. The heme is noncovalently attached, with a maximal, in vitro, heme loading of approximately 30%, for both proteins. CD and fluorescence spectroscopies indicate a well-ordered structure, suggesting the low level of heme loading is probably not due to improperly folded protein. EPR confirmed a five-coordinate, high-spin, ferric resting state for both proteins, indicating one axial amino acid ligand, in contrast to the six-coordinate, low-spin, ferric state of cytochrome b_5. The MCD spectrum confirmed this conclusion for Dap1p and indicated the axial ligand is most likely a tyrosine and not a histidine, or a cysteine; however, an aspartic acid residue could not be conclusively ruled out. Potential axial ligands, which are conserved in all MAPRs, were mutated (Y78F, D118A, and Y138F) and purified to homogeneity. The Y78F and D118A mutants were found to bind heme; however, Y138F did not. This result is consistent with the MCD data and indicates that Tyr138 is most likely the axial ligand to the heme in Dap1p.

Dap1p[1] (damage-associated response protein) from *Saccharomyces cerevisiae* has emerged as a critical protein in sterol synthesis. Deletion of Dap1p from the genome makes yeast more sensitive to the methylating agent, methyl methanesulfonate (MMS) (*1*, *2*). MMS is widely used in yeast for mutagenesis and damage repair studies (*3*) because it causes various types of genomic instability (*4*, *5*). The sensitivity of *dap1*Δ is believed to be due to a lowered activity of the yeast lanosterol demethylase, Erg11p/Cyp51p, because the mutant cells were found to accumulate the ergosterol precursor intermediates, squalene and lanosterol (*2*). A more recent study found that the *dap1*Δ had a much lower Erg11p levels than the wild type, even though the *ERG11* mRNA levels were similar in the *dap1*Δ and wild type, suggesting that Dap1p is important for Erg11p stability (*6*). Consistent with this idea, the MMS sensitivity in *dap1*Δ cells was suppressed by the overexpression of *ERG11*, or by the addition of exogenous heme (*6*). In addition, our lab has found that *dap1*Δ has a severe growth defect under low-iron conditions (*7*). On the basis of the data given above, Dap1p may function in a heme-dependent manner by controlling Erg11p stability whose activity as a P450 enzyme is known to be dependent on a prosthetic heme cofactor.

Dap1p is predicted to be a 17 kDa protein containing a heme domain which is highly homologous to the heme binding domain of cytochrome b_5 and is a member of a highly conserved family of proteins present in all eukaryotes

† This research has been supported by NIH Grant GM56062-06 (T.R.H.), NIH Grant EB02056 (R.A.G.), the Roche Foundation for Anemia Research (C.V.), and NIH Instrument Grant DBI-0217922 (EPR).

* To whom correspondence should be addressed. Phone: (831) 459-5884. Fax: (831) 459-2935. E-mail: tholman@chemistry.ucsc.edu.

‡ Department of Chemistry and Biochemistry, University of California, Santa Cruz.

§ These authors contributed equally to this work.

∥ University of California, Berkeley.

⊥ Department of Environmental Toxicology, University of California, Santa Cruz.

[1] Abbreviations: Dap1p, yeast Dap1 protein; mPGRMC1p, mouse progesterone receptor membrane component-1 protein; mPGRMC1p-H6, C-terminally His-tagged, membrane anchor-truncated mPGRMC1p; MAPR, membrane-associated progesterone binding protein; IZA, inner zone antigen; GST, glutathione *S*-transferase; EPR, electron paramagnetic resonance; MCD, magnetic circular dichroism; CD, circular dichroism; Y78F, Dap1p-Tyr78Phe; D118A, Dap1p-Asp118Ala; Y138F, Dap1p-Tyr138Phe; MMS, methyl methanesulfonate; SEC, size exclusion column; Mb, myoglobin; MALDI-ToF, matrix-assisted laser desorption ionization time-of-flight; FPLC, fast protein liquid chromatography.

10.1021/bi0511585 CCC: $30.25
Published on Web 11/19/2005

FIGURE 1: Alignment of IZA (GenBank accession number CAA06732), mPGRMC1p (GenBank accession number NP_058063), Hpr6.6 (GenBank accession number NP_006658), Dap1p (GenBank accession number Q12091), and the cytochrome b_5 binding motif (pfam00173) using Clustal W version 1.82. Conserved amino acid residues that have been mutated in Dap1p are shaded in black, and the numbers above the sequences correspond to the Dap1p sequence. Axial heme-ligating histidines from cytochrome b_5 are also highlighted, for comparison. The single predicted transmembrane segment is indicated above the residues that are involved. This predication is based on a Kyte−Doolittle hydropathy plot with a window size of 9. Fully conserved residues are marked with asterisks, strongly conserved amino acids with colons, and weakly conserved residues with periods.

(*6*, *8*). This family of proteins was given the name membrane-associated progesterone receptor binding proteins (MAPRs) on the basis of the observation that a porcine member of the MAPR family bound progesterone (*9*). Other members of the MAPR family of proteins include inner zone antigen [IZA, also known as 25-Dx (*10*), VEMA (*11*), and Ratp28 (*12*)], found in the Zona fasciculata of the rat adrenal cortex (*13*), Hpr6.6, a human homologue found in epithelial tissues (*14*), and progesterone receptor membrane component-1 (PGRMC1), found in mouse granulosa cells of developing follicles (*15*). All of these mammalian proteins have nearly identical cytochrome b_5 domains, but slightly different C-termini (Figure 1) (*16*). Recently, both Dap1p and its rat homologue, IZA, have been shown to bind heme when expressed as fusion proteins in *Escherichia coli*. However, their biochemical and spectroscopic characterization is limited to the observation that both fusion proteins display Soret bands at 400 nm, which shift to 420 nm upon reduction with dithionite (*6*, *16*). It is remarkable that these proteins bind heme because the two conserved histidine heme ligands found in cytochrome b_5 are absent in the MAPR protein family (Figure 1). However, the combined genetic and biochemical data discussed above (*6*, *16*), suggest that Dap1p is a heme binding protein, whose heme ligation may be directly related to its function. In this paper, we have investigated the biochemical and spectroscopic properties of heme binding in both Dap1p and its mouse homologue, mPGRMC1p, to determine the nature of the heme ligation and if the manner in which they bind heme is consistent between MAPRs from such evolutionary divergent origins.

MATERIALS AND METHODS

Source of Materials. Restriction endonucleases were obtained from New England BioLabs (Beverly, MA). Hemin, sodium dithionite, and sodium cyanide were purchased from Sigma. All other reagents were reagent grade or better and were used without further purification.

Plasmids and Strains. The *E. coli* protein expression plasmids for Dap1p were constructed as follows. The *DAP1* coding sequence flanked with NcoI (5′) and XhoI (3′) restriction sites was PCR amplified from yeast genomic DNA with two primers (5′-TTTCATGCCATGGGCGAATTCAT-GTCCTTCATTAAAAACTTG-3′ and 5′-CCGCTCGAGT-TAAAGCTTTACGTTCACGCCAGGCTCCGGTTT-3′). The PCR product was subsequently cloned into the pET-28a vector (Novagen), generating the pDap1 plasmid. The *DAP1* gene was verified by DNA sequencing, however, it was determined that Lys145 (AAA) replaced Ile145 (ATT) in multiple PCR products, which is most likely due to a natural variation in the yeast strains.

The *E. coli* protein expression plasmid for the C-terminally His-tagged, truncated mPGRMC1 protein was constructed, essentially as described above; however, the membrane anchor was deleted (residues 1−43). The mouse *PGRMC1* coding sequence flanked by NcoI (5′) and XhoI (3′) restriction sites was PCR amplified from mouse cDNA and cloned into the pET-28a vector, generating the plasmid (pPGRMC1). The *PGRMC1* gene was verified by DNA sequencing and subsequently cut with NcoI and HindIII and ligated into a similarly cut pET-28a plasmid to generate the C-terminally His-tagged, membrane anchor-truncated plasmid (pPGRMC1-H6). The primers used were 5′-CAAGC-CATGGGCGAATTCAAGATCGTTCGCGGGGACCAG-

3′ and 5′-CCGCTCGAGTTAAAGCTTTTCATTCTTCCGAGCTGTCT-3′.

The Dap1p mutants Y78F, D118A, and Y138F were generated by site-directed mutagenesis with pDap1, using a Quikchange kit (Stratagene), and the mutations verified by DNA sequencing.

Expression of Proteins. A single colony of *E. coli* BL21(DE3) bearing either of the above protein expression plasmids was grown in 5 mL of LB broth containing 25 μg/mL kanamycin (FisherBiotech) and reinoculated into 14 L of the same medium. The cultures were grown at 37 °C (225 rpm) until an OD_{600} of 0.6 was attained. Protein expression was induced with IPTG at a concentration of 0.5 mM (FisherBiotech), and cells were grown overnight at 20 °C with 100 rpm shaking.

Purification of Proteins. The wild-type Dap1 protein (Dap1p) was purified as follows. IPTG-induced cells were harvested by centrifugation and washed. The pellet was resuspended in 50 mL of 25 mM HEPES buffer (pH 7.5) containing 10% glycerol, 0.1% Triton X-100, and 150 mM NaCl. The cells were disrupted by three bursts of sonication (45 s) at 4 °C. Debris was removed by centrifugation at 27000*g* for 15 min and the pellet resonicated as described above. Ammonium sulfate was added to the combined supernatants to a concentration of 10%. The solution was centrifuged for 15 min (27000*g*) and the supernatant collected. The supernatant was brought to a concentration of 40% ammonium sulfate and centrifuged as described above, and the pellet was stored at −20 °C. The pellet was resuspended in a minimum amount of Milli-Q water (∼40% ammonium sulfate, final concentration) and loaded directly onto a Macro-Prep methyl hydrophobic column (Bio-Rad), previously equilibrated with 40% ammonium sulfate and 25 mM HEPES (pH 7.5). The column was washed with 3 column volumes of equilibration buffer, and the protein was eluted with a linear gradient of water. Fractions with a heme-to-protein ratio of >1 (A_{398}/A_{280}) were pooled, dialyzed against 25 mM HEPES (pH 7.5), and concentrated in an Amicon pressure concentrator. The concentrated protein was then loaded onto a Superdex-75 gel filtration column (Amersham Biosciences), equilibrated with 25 mM HEPES (pH 7.5), and eluted with the same buffer. It should be noted that two peaks containing Dap1p eluted, one with an approximate size of a tetramer and another which eluted with the void volume (presumably due to a large aggregate of Dap1p). The area of the tetramer Dap1p peak would decrease if the ammonium sulfate was not completely removed from the sample before loading onto the Superdex-75 column. Fractions were checked for purity by 12% SDS−PAGE with gels stained with Coomassie Blue. Greater than 95% pure fractions were pooled and concentrated as described above, for a final yield of 6 mg/L of culture (stored with 5% glycerol at −20 °C). The mutants of Dap1p (Y78F, D118A, and Y138F) were also purified as described above.

Bacteria expressing mPGRMC1p-H6 were grown and lysed in a manner similar to that for Dap1p-expressing cells, described above. The crude lysate was loaded directly onto a Ni−NTA column previously equilibrated with 25 mM HEPES (pH 7.5) and 150 mM NaCl and washed with 2 column volumes of buffer. The protein was eluted with a linear gradient of 500 mM imidazole (250 mM elution for mPGRMC1p-H6). Fractions greater than 95% pure were collected and stored as mentioned above for Dap1p, with a yield of 4 mg/L.

Determination of the Oligomeric State. Purified Dap1p and mPGRMC1p-H6 were loaded onto an analytical Superdex 200 size exclusion column (Amersham Biosciences) with a running buffer of 25 mM HEPES (pH 7.4), with and without 150 mM NaCl. The ATKA FPLC system (Amersham Biosciences) was run at a rate of 0.5 mL/min, and column was pre-equilibrated with running buffer before each run. A standard protein solution (MP Biomedical, Inc.) was used to confirm protein size for Dap1p and mPGRMC1p-H6, which contained apoferritin (480 kDa), γ-globulin (160 kDa), albumin (67 kDa), ovalbumin (45 kDa), chymotrypsin (25 kDa), and cytochrome *c* (13 kDa).

Mass Spectroscopy. Identification of proteins was confirmed on an Ettan MALDI-ToF/Pro instrument (Amersham Biosciences). A one millimeter gel plug was picked from the SDS−PAGE gel by an Ettan Spotpicker (Amersham Biosciences), for both Dap1p and mPGRMC1p-H6. The gel plugs were digested overnight with sequencing grade trypsin (Promega) and the peptides extracted with three washes of 75% acetonitrile and 0.1% TFA. The solvent was removed with a speed-vac, and the peptides were reconstituted in 10 μL of 50% acetonitrile, 0.5% TFA, and 26 mM α-cyano-4-hydroxycinnamic acid. Each peptide solution was spotted twice on the sample slide (0.4 μL) and allowed to dry before analysis. The masses of measured peptides were matched with an Oracle 9i database through the Ettan MALDI-Tof Pro software version 2.0 (Amersham Biosciences).

Electronic Spectroscopy. UV−vis spectra of Dap1p and mPGRMC1p-H6 were taken in 25 mM HEPES (pH 7.5) with a Perkin-Elmer Lamda 40 instrument. All protein samples were reduced by adding excess solid dithionite (10-fold) to the as isolated oxidized samples. Excess cyanide and imidazole (1000-fold each) were added from 7 M stock solutions [in 25 mM HEPES (pH 7.5)] to the oxidized proteins to supply exogenous ligands to the iron.

Percent Heme Loading and Determination of ϵ of the Soret Band. The percent of heme loading of Dap1p and mPGRMC1p-H6 was determined by the pyridine hemochrome assay (*17*, *18*). Briefly, 75 μL of 1 N NaOH, 175 μL of pyridine, and ∼2 mg of dithionite were added to 750 μL of protein (less than 4 μM), and the solution was monitored at 418 nm. The heme concentration was determined utilizing an extinction coefficient of 191.5 mM^{-1} cm^{-1} at 418 nm for the pyridine−heme adduct. The heme concentration determined for Dap1p and mPGRMC1p-H6 by the pyridine hemochrome assay were then used to determine their Soret band extinction coefficients. Horse heart myoglogin (Mb) (Sigma) was used as standard for both the pyridine hemochrome assay and the extinction coefficient of the Soret band determination (170 mM^{-1} cm^{-1} at 408 nm) (*19*). Protein concentrations were independently determined by the Bradford assay using a horse heart Mb standard.

Reconstitution of Heme. Reconstitution of Dap1p was performed with the following procedure (*20*, *21*). A 1 mL protein solution (1 mg/mL) in 50 mM sodium phosphate buffer (pH 7.0) was added to a three-necked flask and degassed by purging nitrogen for 2−3 h. In a separate round-bottom flask, a 10 mM solution of hemin in dimethyl sulfoxide (DMSO) was prepared. This hemin solution was degassed, and 1.1 equiv of hemin was added to the protein

solution. DTT was added to a final concentration of 5 mM, using a 0.5 M stock solution, and then a 300-fold excess of solid dithionite to protein was added and the solution kept in the dark overnight at room temperature. The protein was separated from uncomplexed heme with a Sephadex G25 column equilibrated with 50 mM sodium phosphate buffer (pH 7.0) at 4 °C. Reconstitution of Dap1p with ferric heme was also attempted, where the ferric heme was dissolved in DMSO and titrated into the buffered protein solution at a minimal volume (*20*).

Determination of Heme Covalency. Dap1p and mPGRMC1p-H6 were digested overnight at 37 °C with sequencing grade trypsin (Promega), and bovine cytochrome *c* was digested as a standard (*22*). A 100 μL aliquot of the digested protein solutions was loaded on a C4, 300A 4.6 mm × 150 mm column (Western Analytical Products, Inc.) and separated with a step gradient of 62% H_2O in 0.1% TFA (w/v) and 38% acetonitrile in 0.1% TFA (w/v). Free hemin eluted at 16 min.

Circular Dichroism (CD) and Fluorescence Spectroscopy. Far-UV spectra of purified Dap1p were obtained on AVIV 60DS CD spectrophotometer. Spectra were recorded using a cuvette with a 0.1 mm path length from 250 to 190 nm with a step size of 1 nm and an averaging time of 10 s at room temperature. For all spectra, an average of six scans were obtained and the background spectra of the buffer were subtracted.

The tryptophan fluorescence spectra were recorded with a Perkin-Elmer LS 50B luminescence spectrometer. Dap1p (10 μM) was excited at 295 nm, and the emission was scanned from 330 to 400 nm in 50 mM phosphate buffer solution (pH 7.0).

EPR Spectroscopy. The EPR spectra of Dap1p (8 mg/mL) and mPGRMC1p-H6 (10.4 mg/mL), all in 25 mM HEPES (pH 7.5), were recorded with a Bruker Elexsys/Oxford Cryostat EPR instrument (0−8000 G, 8 G modulation amplitude, 0.2 mW, 9.63 GHz, and 4 K). Sodium cyanide and imidazole were added to the individual samples (1 μL of a 7 M stock solutions) to produce a final concentration of 35 mM. Horse heart Mb (Sigma) was used as a standard (0.4 mg/mL).

Magnetic Circular Dichroism (MCD) Measurements. MCD measurements were taken at 22 °C on an 62DS circular dichroism spectrophotometer (Aviv, Lakewood, NJ) equipped with a 0.64 T permanent magnet (model PM-2, Jasco, Eaton, MD). Samples of Dap1p, Y78F, and D118A, containing heme concentrations of 80, 100, and 70 μM, respectively, in 25 mM HEPES buffer (pH 7.5), were placed in a 1 mm path length cylindrical quartz cell. MCD spectra were calculated from the difference between parallel and antiparallel field measurements, baseline corrected, and smoothed (23-point Savitzky−Golay algorithm).

RESULTS AND ANALYSIS

Expression and Purification. Dap1p, Y78F, D118A, Y138F, and mPGRMC1p-H6 were expressed in an *E. coli* strain (BL21-DE3) at high levels. Dap1p, Y78F, D118A, and Y138F were purified by ammonium sulfate precipitation, a hydrophobic column, and a gel filtration column for a final yield of approximately 6 mg/L. mPGRMC1p-H6 was purified by a Ni−NTA agarose affinity column for a yield of approximately 4 mg/L.

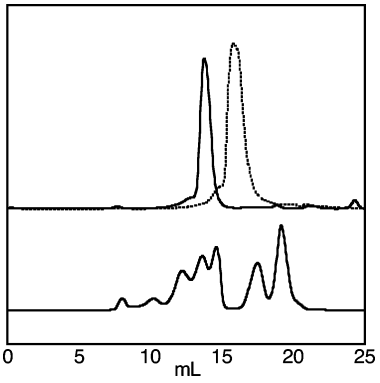

FIGURE 2: HPLC traces of the analytical size exclusion column. Top traces are that of Dap1p (solid line, no salt) and Dap1p (dashed line, 150 mM salt). The bottom trace is that of protein standards. The first peak is the void volume, and then apoferritin (480 kDa), γ-globulin (160 kDa), albumin (67 kDa), ovalbumin (45 kDa), chymotrypsin (25 kDa), and cytochrome *c* (13 kDa).

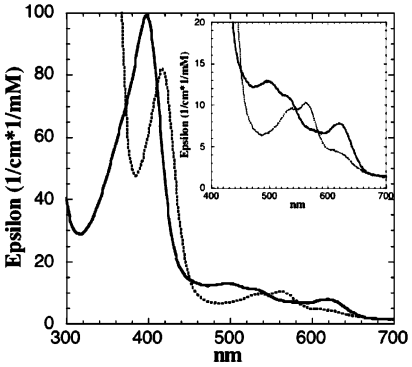

FIGURE 3: UV−visible spectra of oxidized (—) and reduced (•••) Dap1p. The inset is an enhancement of the far-visible spectrum. The large absorbance at 300 nm for the reduced spectrum is that of excess sodium dithionite.

Determination of the Oligomeric State of Dap1p. Dap1p appeared to run as a multimer on the Superdex 75 column during purification; therefore, purified Dap1p and mPGRMC1p-H6 samples were analyzed on an analytical Superdex 200 size exclusion column (SEC) to measure their as isolated size more accurately. Initial analysis of purified Dap1p and mPGRMC1p-H6 in 25 mM HEPES (pH 7.4) showed a single peak at ~68 kDa (a possible tetramer), as compared to protein standards (Figure 2). Addition of DTT, CHAPS, or Triton-X caused an aggregation of Dap1p to a large multimer between 480 and 160 kDa. Addition of 150 mM NaCl to Dap1p, however, reduced the tetramer to a dimer, which ran as ~34 kDa (Figure 2). Addition of excess DTT to Dap1p could not reduce the dimer to a monomer on the analytical SEC.

Mass Spectroscopy. Samples of SDS−PAGE-isolated, trypsin-digested Dap1p and mPGRMC1p-H6 were identified by MALDI-ToF. Both of their expectation values were 0.000, and their coverage was greater than 55%. Seven of 22 peaks and six of 16 were assigned to expected peptides of Dap1p and mPGRMC1p-H6, respectively.

Electronic Spectroscopy. The UV−visible spectra of Dap1p (Figure 3) display maxima at 398 nm, characteristic of a hemoprotein Soret band, with three additional bands at 500, 530, and 620 nm (mPGRMC1p-H6 shows the same absorption spectra, data not shown). The small peak near 620 nm has been designated as the charge-transfer band

between the heme and the high-spin Fe(III) (*23*). Upon reduction with excess dithionite, the Soret bands from both Dap1p and mPGRMC1p-H6 underwent a red shift to 418 nm, with two new bands at 538 and 562 nm, corresponding to the β and α heme bands, respectively. These data are consistent with a high-spin, five-coordinate ferric heme center for both Dap1p and mPGRMC1p-H6, as isolated (*24*−*26*). Addition of imidazole to the ferric heme protein shifts the Soret band from 398 to 407 nm and decreases the intensity of the 620 nm band for Dap1p. Addition of excess CN^- to the solution of Dap1p gave rise to a red-shifted Soret band (from 398 to 421 nm) and an additional broad band at 545 nm. These changes in the electronic spectra are consistent with both imidazole and CN^- binding directly to the iron, generating a six-coordinate, low-spin Fe(III) (*27*, *28*).

Percent Heme Loading and Determination of ϵ of the Soret Band. The pyridine hemochrome assay determined the heme content of Dap1p to be 17% (highest value of three purifications) and that of mPGRMC1p-H6 to be 21% (highest value of three purifications) (*17*, *18*). The heme loadings for the Dap1p mutants were as follows: 7% for Y78F, 25% for D118A, and 0% for Y138F (highest value of two purifications). Utilizing the pyridine hemochrome assay, the extinction coefficients of the Soret band at 398 nm were calculated to be 99 ± 4.1 and 102 ± 3.5 mM^{-1} cm^{-1} for Dap1p and mPGRMC1p-H6, respectively. The extinction coefficient values of the heme $\pi \rightarrow \pi^*$ Soret transition for Dap1p and mPGRMC1p-H6 are close to the lower limit of the values described in the literature for hemoproteins (100−200 mM^{-1} cm^{-1}) (*29*).

Reconstitution of Heme. Reconstitution of the 17% heme-loaded Dap1p with ferrous heme increased the heme content to a maximum of 27%, while reconstitution with ferric heme was unsuccessful in increasing the heme content of Dap1p. Reconstitution under buffer conditions where Dap1p was a dimer (150 mM salt) also did not improve the percent loading of heme. Reconstitution was attempted under various other conditions such as varying pH and denaturant (urea and guanidinium HCl) with no success.

Heme Covalency. Dap1p and mPGRMC1p-H6 were both digested with trypsin, and their fragments were separated by HPLC, with the peptide backbone (215 nm), aromatic side chains (280 nm), and heme (400 nm) monitored simultaneously. Only one peak was detected at 400 nm and eluted at 16 min for both Dap1p and mPGRMC1p-H6. This corresponds to the elution time for free heme and indicates the heme is not covalently attached to Dap1p or mPGRMC1p-H6. This result differs from that of the control, cytochrome *c*, which displayed a protein−heme peak that eluted at 14 min (*22*).

Circular Dichroism (CD) and Fluorescense Spectroscopy. The far-UV CD spectra of Dap1p exhibit characteristic features near 222, 208, and 192 nm with a 190 nm/222 nm ratio of 1.6, which indicate that the protein has α-helical secondary structure (*30*). In the fluorescence spectra of Dap1p, the tryptophan maxima were observed at 341 nm, indicating that the tryptophans of Dap1p are partially buried. For comparison, free, solvent-exposed tryptophan gave a maximum of 355 nm.

EPR Spectroscopy. Dap1p, mPGRMC1p-H6, and heme-reconstituted Dap1p all display identical EPR spectra, with a strong derivative signal centered at a *g* of ∼6 (*g* values of 6.40 and 5.59) and a smaller negative signal with a *g* of 1.99, which clearly indicate an axial Fe(III) high-spin species (E/D = 0.017) (Figure 4). The signals of both Dap1p and mPGRMC1p-H6 were integrated by comparing the signal area with that of a similar heme concentration of horse heart Mb, which confirmed the approximate heme content determined by the pyridine hemochrome assay (the zero-field splittings of Dap1p and mPGRMC1p-H6 were assumed to be comparable to that of myoglobin). Addition of excess CN^- gave EPR signals with *g* values of 2.97 and 2.22 for Dap1p and 2.90 and 2.23 for mPGRMC1p-H6. Addition of excess imidazole to Dap1p gave an EPR spectrum with *g* values of 2.26 and 2.96, whereas the two *g* values for mPGRMC1p-H6 were 2.26 and 2.98 (the third *g* value for both the imidazole and cyanide adducts was distorted by a minor copper impurity at $g = 2$).

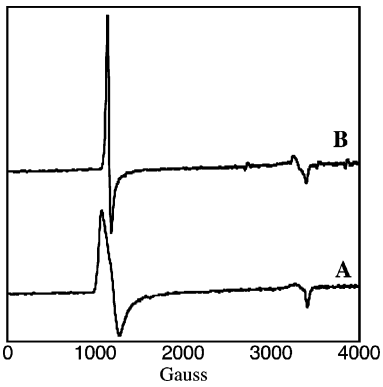

FIGURE 4: EPR spectra of (A) Dap1p (8 mg/mL, HEPES, pH 7.5) and (B) horse heart myoglobin (0.4 mg/mL, HEPES, pH 7.5). EPR parameters: 0−8000 G, 8 G modulation amplitude, 0.2 mW, 9.63 GHz, and 4 K.

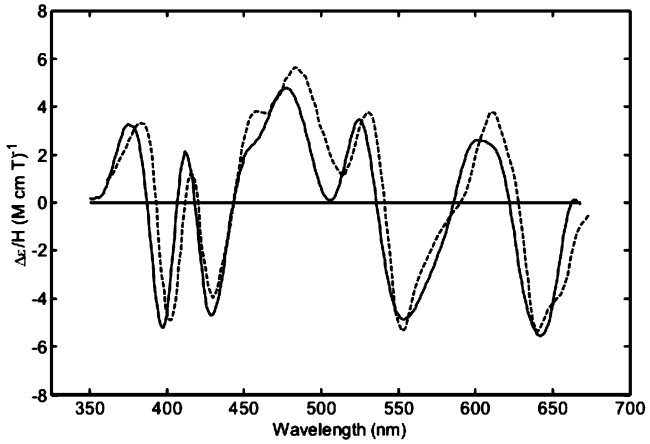

FIGURE 5: MCD spectra of ferric Dap1p in 25 mM HEPES buffer (pH 7.5) at 22 °C (—) and ferric bovine liver catalase in 100 mM potassium phosphate buffer (pH 7.0) at 14 °C (- - -). The catalase spectrum was taken from ref *47*.

MCD Spectroscopy. The MCD spectrum of ferric Dap1p in the Soret and visible band spectral regions (Figure 5) contains several features providing a "fingerprint" that can aid in characterizing the nature of the heme axial ligand. A "W"-shaped feature of modest intensity (magnitudes of 3−5 M^{-1} cm^{-1} T^{-1}) in the Soret region contains troughs at 397 and 429 nm separated by a central peak at 412 nm and is bordered on the lower-wavelength side by a peak at 376 nm. In the visible region, peaks at 478, 525, and 604 nm are interlaced with troughs at 505, 555, and 643 nm. The spectra

of Y78F and D118A were comparable to that of Dap1p, with only negligible differences.

DISCUSSION

Dap1p has recently been shown to bind heme and is apparently critical to Erg11p stability; however, its physiological role remains undetermined (*6*). Work by others and our unpublished biological studies indicate that Dap1p may function in a heme-dependent mechanism (*6*, *7*). As part of our ongoing effort to determine the role of Dap1p and its mechanism of action, we expressed and purified Dap1p and its mouse homologue, mPGRMC1p-H6, and conducted biochemical investigations in the hope of shedding some light on their specific biological function. In this regard, our investigations have revealed several novel aspects about how Dap1p and mPGRMC1p-H6 may function. First, we have found that Dap1p is a dimer at physiological salt concentrations, similar to that observed for IZA (*16*), but it has a propensity to form tetramers at lower salt concentrations. Second, both Dap1p and mPGRMC1p-H6 bind heme noncovalently. Considering that IZA also binds heme and there is 98% sequence homology between mPGRMC1p and IZA and 57% sequence homology between Dap1p and IZA, heme binding appears to be a common characteristic to this family of proteins. Third, Dap1p and mPGRMC1p-H6 bind heme with a low loading percentage, 17 and 21%, respectively, suggesting the low heme content may also be a common trait of this novel protein family. The heme loading percentage for Dap1p can be increased to 27% by incubation with ferrous heme and is independent of the multimeric state of the protein (i.e., dimer vs tetramer). The low heme content for Dap1p and mPGRMC1p-H6 is most likely not due to their expression in *E. coli* since other hemoproteins can be fully loaded with heme (*31*−*33*), or due to misfolded protein since both CD and fluorescence spectroscopy indicate Dap1p has a well-ordered structure. This low heme content in a well-ordered protein is notable because of the similarity of Dap1p's sequence to that of cytochrome b_5, a tight heme binding protein with two His ligands to the heme. Considering that these proximal histidine ligands are not conserved in Dap1p, it is clear that Dap1p binds heme with axial ligand(s) other than cytochrome b_5, which could explain its low heme loading. Interestingly, the NMR structure of a plant MAPR, At2g24940.1, did not have heme bound even though there was a cleft for potential heme binding in the structure (*34*). The lack of heme binding could be explained by the fact that the protein was expressed in vitro with wheat germ extract, which would not provide a heme cofactor for binding.

The electronic spectra of both Dap1p and mPGRMC1p-H6 in the oxidized and reduced states indicate a high spin, five-coordinate heme environment, in contrast to the low-spin, six-coordinate heme environment found in cytochrome b_5 (*24*, *25*). In terms of both absorption peak position and amplitudes in the Soret, α/β, and charge-transfer transitions, the optical spectra of Dap1p and mPGRMC1p-H6 are similar to those of both histidine-ligated proteins (i.e., metmyoglobin and prostaglandin H synthase) and tyrosine-ligated proteins (i.e., catalase) (*27*), which makes it difficult to determine the nature of the axial ligand. A low-spin, six-coordinate species could be generated for both Dap1p and mPGRMC1p-H6 with the addition of cyanide and imidazole, as seen by the change in UV−vis spectra, indicating either an empty coordination site or an easily displaced ligand, such as exogenous water. The high-spin, five-coordinate ligand environment for ferric Dap1p and mPGRMC1p-H6 is corroborated by its EPR spectrum, which manifests an axial, ferric signal (E/D = 0.017). The E/D value and rhombicity index, R [$R = (\Delta g/16) \times 100 = 5.1\%$, where Δg is the absolute difference between the two g values centered at $g = 6$], for both Dap1p and mPGRMC1p-H6 are very similar to the signals of horseradish peroxidase (pH 8.1) (*35*) and cytochrome-*c* peroxidase (pH 5) (*36*), suggesting an axial His and a bound water (or open coordination site). The assignment of an axial His is supported by the low-spin, EPR signal observed after addition of exogenous imidazole (g values of 2.26 and 2.96), similar to that observed for hemoglobin (*37*). Nevertheless, this analysis is in contrast with the fact that there are no conserved histidines in the MAPR protein family that could function as the axial ligand in Dap1p or mPGRMC1p-H6. Considering that the rhombicity index is a poor indicator of the axial ligation (*27*) and that the added imidazole could possibly displace the endogenous axial ligand, generating a bis-imidazolate complex, another spectroscopic method was required to identify the nature of the axial ligand.

MCD spectroscopy is an extremely sensitive method of investigating heme proteins and provides more reliable information about the heme state and axial ligands than EPR or simple optical spectra (*38*, *39*). Coordination differences, while not apparent in the UV−vis absorption spectra, are more obvious from the differences in their respective MCD spectra. MCD spectra can have negative and positive absorptions, which provide considerably more fine structure than can be seen in absorption spectra alone. Therefore, empirical comparisons of MCD spectra contain twice the information (i.e., intensity and sign) and thus provide better fingerprints than UV−vis absorption alone. In this regard, the MCD spectrum of Dap1p is clearly not consistent with histidine as the axial ligand, lacking the more intense "S"-shaped feature centered near 412 nm as seen in the spectra of both ferric myoglobin, having a histidine residue as the fifth ligand and water as the sixth (peak amplitude of 14 M^{-1} cm^{-1} T^{-1}) (*40*, *41*), and ferric cytochrome b_5, having bis-histidine axial coordination (peak amplitude of 68 M^{-1} cm^{-1} T^{-1}) (*42*). Nor does the spectrum of Dap1p resemble the spectrum observed in high-spin ferric horseradish peroxidase, which has proximal histidine coordination without a water as the sixth ligand (*41*). The spectrum is also not consistent with cysteine ligation due to the absence of the prominent, single trough at 395 nm (peak amplitude of −25 M^{-1} cm^{-1} T^{-1}) (*43*). The MCD spectrum of Dap1p is more consistent in the visible region with spectra observed in heme proteins (*44*) and model compounds (*45*) having carboxylate heme coordination, but their Soret region spectral features do not correspond well with the Dap1p spectrum. For example, the central Soret peak of heme oxygenase H25A (assigned heme-glutamate coordination) is red-shifted by 20 nm to 392 nm and the short-wavelength trough is red-shifted by 40 nm to 358 nm when compared with the corresponding features in Dap1p (*44*). However, a remarkably close match to both the Soret and visible band MCD of Dap1p is found in the MCD of the catalases, a family of heme proteins that catalyze the disproportionation of hydrogen peroxide and have an axial tyrosine ligation (Figure 5) (*46*−*49*). X-ray

crystallography of bovine liver catalase shows not only that the heme is axially coordinated by a tyrosine residue (presumably in the form of tyrosinate) but also that the tyrosine hydroxyl oxygen is hydrogen bonded by a nearby arginine residue (*50*). It is tempting to speculate that the presence of this hydrogen bond to the heme axial ligand may explain why the MCD spectra of the catalases are distinguished from those of other tyrosine−heme coordinated examples lacking this hydrogen bond, such as Mb H93Y or heme−phenolate model compounds (*44*, *51*).

As stated previously, the MAPR family of proteins does not contain the conserved histidine ligands of cytochrome b_5, but they do have a conserved tyrosine and aspartic acid adjacent to the histidine positions of cytochrome b_5 (Tyr78 and Asp118 in Figure 1). These two candidates for ligation were subsequently mutated (Y78F and D118A); however, both mutant proteins still bound heme, and there was minimal change in their MCD spectra compared to those of Dap1p. We therefore considered other conserved tyrosine residues as potential axial ligands, and one, Y138F, had no bound heme after purification. These results indicate that Tyr138 is the axial ligand to the heme for Dap1p, confirming the MCD spectroscopy results. If one assumes the structure of Dap1p is comparable to the NMR structure of its plant homologue, At2g24940.1 (63% similar sequence), one observes that the conserved tyrosine (Tyr138 in Dap1p and Tyr92 in At2g24940.1) is positioned on the edge of the hydrophobic cleft and could potentially bind a heme cofactor. Considering that this tyrosine is conserved in all MAPRs, it is highly likely that this tyrosine is the axial ligand for both mPGRMC1 (Tyr164) and IZA (Tyr164), as well. Interestingly, there is a conserved lysine adjacent to this tyrosine, which could hydrogen bond and account for the "catalase-like" MCD spectrum.

The biological function(s) of MAPR proteins is still unclear with regard to heme (*6*, *16*) and/or sterol (*9*, *10*) binding. The most extensive data to date comes from the study of the yeast MAPR, Dap1p, which support a role for heme binding in its biological function. The fact that the sequence of Dap1p is highly homologous with that of cytochrome b_5 but ligates heme in a different manner may also have relevance to its biological function. Previously, it was observed that exogenous heme in the yeast media can correct the *dap1*Δ phenotype and restore the Erg11p levels (*6*); however, as yeast can degrade heme and release iron via heme oxygenase (Hmx1p), this experiment cannot differentiate between heme and iron. In this study, mutating Asp91 in Dap1p, a conserved residue in all MAPR and cytochrome b_5 proteins, abolished heme binding in Dap1p and did not complement the MMS sensitivity phenotype of the *dap1*Δ strain. This result was interpreted as meaning that heme binding was critical to Dap1p function; however, it should be noted that the Asp91 mutant was not conclusively proven to be properly folded while attached to the GST fusion protein (*6*). In addition, the amount of Erg11p was lowered in the *dap1*Δ strain, but the transcription of *ERG11* was not, indicating that Dap1p does not play a role in transcriptional activation. On the basis of the data reported here and in the literature, there are two probable roles for Dap1p with heme. First, Dap1p might play a role in cellular heme synthesis or transport, thereby indirectly affecting Erg11p levels. Consistent with this idea, the *dap1*Δ mutant has a transcriptional profile similar to that of heme synthesis pathway mutants (*7*). Another possibility is that Dap1p may play a role as a heme chaperone to Erg11p, thus modulating the stability of Erg11p by delivering its essential cofactor, heme, and consequently increasing its activity in sterol synthesis. The existence of apo-Dap1p along with heme-bound Dap1p under physiological conditions may allow Dap1p to function as a "Heme-stat" to gauge cellular heme status and in turn modulate the Erg11p level and its activity. Mallory et al. did not detect a physical interaction between Dap1p and Erg11p by immunoprecipitation; however, this negative result could be due to the fact that the Dap1p−Erg11p interaction is transient, similar to the interaction between the copper chaperone, Atx1p, and its target, Ccc2p, in yeast (*52*). Both of these possible roles of heme and Dap1p are currently being investigated.

In summary, the current data indicate that both Dap1p and mPRGMC1-H6 bind heme in a similar five-coordinate manner, with tyrosine as the axial ligand (Tyr138 for Dap1p), but they are not 100% loaded with heme. Given the fact that we now have identified the exact axial ligand for Dap1p, we are currently conducting both genetic and biochemical studies to investigate the biological roles of Dap1p and mPGRMC1p and whether heme binding is critical for their function as suggested in the literature.

ACKNOWLEDGMENT

We acknowledge Prof. M. Jurica for the use of her analytical SEC, Prof. Brian Gibney for valuable discussions, and Kate Chabarek, Micheal Eklund, and Pilgrim Jackson for valuable assistance.

REFERENCES

1. Begley, T. J., Rosenbach, A. S., Ideker, T., and Samson, L. D. (2002) Damage recovery pathways in *Saccharomyces cerevisiae* revealed by genomic phenotyping and interactome mapping, *Mol. Cancer Res. 1*, 103−12.
2. Hand, R. A., Jia, N., Bard, M., and Craven, R. J. (2003) *Saccharomyces cerevisiae* Dap1p, a novel DNA damage response protein related to the mammalian membrane-associated progesterone receptor, *Eukaryotic Cell 2*, 306−17.
3. Game, J. C. (2000) The *Saccharomyces* repair genes at the end of the century, *Mutat. Res. 451*, 277−93.
4. Myung, K., and Kolodner, R. D. (2002) Suppression of genome instability by redundant S-phase checkpoint pathways in *Saccharomyces cerevisiae*, *Proc. Natl. Acad. Sci. U.S.A. 99*, 4500−7.
5. Prakash, S., and Prakash, L. (1977) Increased spontaneous mitotic segregation in MMS-sensitive mutants of *Saccharomyces cerevisiae*, *Genetics 87*, 229−36.
6. Mallory, J. C., Crudden, G., Johnson, B. L., Mo, C., Pierson, C. A., Bard, M., and Craven, R. J. (2005) Dap1p, a heme-binding protein that regulates the cytochrome P450 protein Erg11p/Cyp51p in *Saccharomyces cerevisiae*, *Mol. Cell. Biol. 25*, 1669−79.
7. Vulpe, C., and Oh, E. (2005) unpublished results.
8. Mifsud, W., and Bateman, A. (2002) Membrane-bound progesterone receptors contain a cytochrome b_5-like ligand-binding domain, *Genome Biol. 3*, 1−5.
9. Meyer, C., Schmid, R., Schmieding, K., Falkenstein, E., and Wehling, M. (1998) Characterization of high affinity progesterone-binding membrane proteins by anti-peptide antiserum, *Steroids 63*, 111−6.
10. Krebs, C. J., Jarvis, E. D., Chan, J., Lydon, J. P., Ogawa, S., and Pfaff, D. W. (2000) A membrane-associated progesterone-binding protein, 25-Dx, is regulated by progesterone in brain regions involved in female reproductive behaviors, *Proc. Natl. Acad. Sci. U.S.A. 97*, 12816−21.
11. Runko, E., Wideman, C., and Kaprielian, Z. (1999) Cloning and expression of VEMA: A novel ventral midline antigen in the rat CNS, *Mol. Cell. Neurosci. 14*, 428−43.

12. Nolte, I., Jeckel, D., Wieland, F. T., and Sohn, K. (2000) Localization and topology of ratp28, a member of a novel family of putative steroid-binding proteins, *Biochim. Biophys. Acta 1543*, 123−30.
13. Raza, F. S., Takemori, H., Tojo, H., Okamoto, M., and Vinson, G. P. (2001) Identification of the rat adrenal zona fasciculata/reticularis specific protein, inner zone antigen (IZAg), as the putative membrane progesterone receptor, *Eur. J. Biochem. 268*, 2141−7.
14. Hand, R. A., and Craven, R. J. (2003) Hpr6.6 protein mediates cell death from oxidative damage in MCF-7 human breast cancer cells, *J. Cell. Biochem. 90*, 534−47.
15. Peluso, J. J., Pappalardo, A., Losel, R., and Wehling, M. (2005) Expression and function of PAIRBP1 within gonadotropin-primed immature rat ovaries: PAIRBP1 regulation of granulosa and luteal cell viability, *Biol. Reprod. 73*, 261−70.
16. Min, L., Takemori, H., Nonaka, Y., Katoh, Y., Doi, J., Horike, N., Osamu, H., Raza, F. S., Vinson, G. P., and Okamoto, M. (2004) Characterization of the adrenal-specific antigen IZA (inner zone antigen) and its role in the steroidogenesis, *Mol. Cell. Endocrinol. 215*, 143−8.
17. Paul, K. G., Theorell, H., and Akeson, A. (1953) The molar light absorption of pyridine ferroprotoporphyrin, *Acta Chem. Scand. 7*, 1284−7.
18. Furhrhop, J.-H., and Smith, K. M. (1975) *Laboratory Methods in Porphyrin and Metalloporphyrin Research*, Elsevier Scientfic Publishing Co., Amersterdam.
19. Blum, O., Haiek, A., Cwikel, D., Dori, Z., Meade, T. J., and Gray, H. B. (1998) Isolation of a myoglobin molten globule by selective cobalt(III)-induced unfolding, *Proc. Natl. Acad. Sci. U.S.A. 95*, 6659−62.
20. Daltrop, O., Stevens, J. M., Higham, C. W., and Ferguson, S. J. (2002) The CcmE protein of the c-type cytochrome biogenesis system: Unusual in vitro heme incorporation into apo-CcmE and transfer from holo-CcmE to apocytochrome, *Proc. Natl. Acad. Sci. U.S.A. 99*, 9703−8.
21. Stevens, J. M., Daltrop, O., Higham, C. W., and Ferguson, S. J. (2003) Interaction of heme with variants of the heme chaperone CcmE carrying active site mutations and a cleavable N-terminal His tag, *J. Biol. Chem. 278*, 20500−6.
22. Schulz, H., Hennecke, H., and Thony-Meyer, L. (1998) Prototype of a heme chaperone essential for cytochrome *c* maturation, *Science 281*, 1197−200.
23. Bartalesi, I., Bertini, I., Ghosh, K., Rosato, A., and Turano, P. (2002) The unfolding of oxidized c-type cytochromes: The instructive case of *Bacillus pasteurii*, *J. Mol. Biol. 321*, 693−701.
24. Lever, A. B. P., and Gray, H. B. (1983) *Iron Porphyrins, Part 1*, Addison-Wesley Publishing Co., Reading, MA.
25. Pettigrew, G. W., and Moore, G. R. (1987) *Cytochrome c, Biological Aspects*, Springer-Verlag, Berlin.
26. Smulevich, G., Neri, F., Willemsen, O., Choudhury, K., Marzocchi, M. P., and Poulos, T. L. (1995) Effect of the His175 → Glu mutation on the heme pocket architecture of cytochrome *c* peroxidase, *Biochemistry 34*, 13485−90.
27. Tsai, A. L., Kulmacz, R. J., Wang, J. S., Wang, Y., Van Wart, H. E., and Palmer, G. (1993) Heme coordination of prostaglandin H synthase, *J. Biol. Chem. 268*, 8554−63.
28. Kulmacz, R. J., Tsai, A. L., and Palmer, G. (1987) Heme spin states and peroxide-induced radical species in prostaglandin H synthase, *J. Biol. Chem. 262*, 10524−31.
29. Moore, G. R., and Pettigrew, G. W. (1990) *Cytochromes c: Evolutionary Structural and Physicochemical Aspects*, Springer-Verlag, Berlin.
30. Padmanabhan, S., Marqusee, S., Ridgeway, T., Laue, T. M., and Baldwin, R. L. (1990) Relative helix-forming tendencies of nonpolar amino acids, *Nature 344*, 268−70.
31. Beck von Bodman, S., Schuler, M. A., Jollie, D. R., and Sligar, S. G. (1986) Synthesis, bacterial expression, and mutagenesis of the gene coding for mammalian cytochrome b_5, *Proc. Natl. Acad. Sci. U.S.A. 83*, 9443−7.
32. Arnesano, F., Banci, L., Bertini, I., and Felli, I. C. (1998) The solution structure of oxidized rat microsomal cytochrome b_5, *Biochemistry 37*, 173−84.
33. Bertini, I., Luchinat, C., Turano, P., Battaini, G., and Casella, L. (2003) The magnetic properties of myoglobin as studied by NMR spectroscopy, *Chemistry 9*, 2316−22.
34. Song, J., Vinarov, D., Tyler, E. M., Shahan, M. N., Tyler, R. C., and Markley, J. L. (2004) Hypothetical protein At2g24940.1 from *Arabidopsis thaliana* has a cytochrome b_5 like fold, *J. Biomol. NMR 30*, 215−8.
35. Blumberg, W. E., Peisach, J., Wittenberg, B. A., and Wittenberg, J. B. (1968) The electronic structure of protoheme proteins. I. An electron paramagnetic resonance and optical study of horseradish peroxidase and its derivatives, *J. Biol. Chem. 243*, 1854−62.
36. Wittenberg, B. A., Kampa, L., Wittenberg, J. B., Blumberg, W. E., and Peisach, J. (1968) The electronic structure of protoheme proteins. II. An electron paramagnetic resonance and optical study of cytochrome *c* peroxidase and its derivatives, *J. Biol. Chem. 243*, 1863−70.
37. Ikeda-Saito, M., and Iizuka, T. (1975) Studies on the heme environment of horse heart ferric cytochrome *c*. Azide and imidazole complexes of ferric cytochrome *c*, *Biochim. Biophys. Acta 393*, 335−42.
38. Sutherland, J. C., and Holmquist, B. (1980) Magnetic circular dichroism of biological molecules, *Annu. Rev. Biophys. Bioeng. 9*, 293−326.
39. Hatano, M., and Nozawa, T. (1978) Magnetic circular dichroism approach to hemoprotein analyses, *Adv. Biophys. 11*, 95−149.
40. Vickery, L., Nozawa, T., and Sauer, K. (1976) Magnetic circular dichroism studies of myoglobin complexes. Correlations with heme spin state and axial ligation, *J. Am. Chem. Soc. 98*, 343−50.
41. Dawson, J. H., Kadkhodayan, S., Zhuang, C., and Sono, M. (1992) On the use of iron octa-alkylporphyrins as models for protoporphyrin IX-containing heme systems in studies employing magnetic circular dichroism spectroscopy, *J. Inorg. Biochem. 45*, 179−92.
42. Vickery, L., Salmon, A., and Sauer, K. (1975) Magnetic circular dichroism studies on microsomal aryl hydrocarbon hydroxylase: Comparison with cytochrome b-5 and cytochrome P-450-cam, *Biochim. Biophys. Acta 386*, 87−98.
43. Sono, M., Stuehr, D. J., Ikeda-Saito, M., and Dawson, J. H. (1995) Identification of nitric oxide synthase as a thiolate-ligated heme protein using magnetic circular dichroism spectroscopy. Comparison with cytochrome P-450-CAM and chloroperoxidase, *J. Biol. Chem. 270*, 19943−8.
44. Pond, A. E., Roach, M. P., Sono, M., Rux, A. H., Franzen, S., Hu, R., Thomas, M. R., Wilks, A., Dou, Y., Ikeda-Saito, M., Ortiz de Montellano, P. R., Woodruff, W. H., Boxer, S. G., and Dawson, J. H. (1999) Assignment of the heme axial ligand(s) for the ferric myoglobin (H93G) and heme oxygenase (H25A) cavity mutants as oxygen donors using magnetic circular dichroism, *Biochemistry 38*, 7601−8.
45. Nozawa, T., Ookubo, S., and Hatano, M. (1980) Visible and near-infrared MCD spectra of h.s. iron(III) complexes of protoporhyrin-IX-dimethylester, *J. Inorg. Biochem. 12*, 253−67.
46. Abraham, B. D., Sono, M., Boutaud, O., Shriner, A., Dawson, J. H., Brash, A. R., and Gaffney, B. J. (2001) Characterization of the coral allene oxide synthase active site with UV−visible absorption, magnetic circular dichroism, and electron paramagnetic resonance spectroscopy: Evidence for tyrosinate ligation to the ferric enzyme heme iron, *Biochemistry 40*, 2251−9.
47. Andersson, L. A., Johnson, A. K., Simms, M. D., and Willingham, T. R. (1995) Comparative analysis of catalases: Spectral evidence against heme-bound water for the solution enzymes, *FEBS Lett. 370*, 97−100.
48. Eglinton, D. G., Gadsby, P. M., Sievers, G., Peterson, J., and Thomson, A. J. (1983) A comparative study of the low-temperature magnetic circular dichroism spectra of horse heart metmyoglobin and bovine liver catalase derivatives, *Biochim. Biophys. Acta 742*, 648−58.
49. Browett, W. R., and Stillman, M. J. (1979) Magnetic circular dichroism studies of bovine liver catalase, *Biochim. Biophys. Acta 577*, 291−306.
50. Fita, I., and Rossmann, M. G. (1985) The active center of catalase, *J. Mol. Biol. 185*, 21−37.
51. Roach, M. P., Puspita, W. J., and Watanabe, Y. (2000) Proximal ligand control of heme iron coordination structure and reactivity with hydrogen peroxide: Investigations of the myoglobin cavity mutant H93G with unnatural oxygen donor proximal ligands, *J. Inorg. Biochem. 81*, 173−82.
52. Pufahl, R. A., Singer, C. P., Peariso, K. L., Lin, S. J., Schmidt, P. J., Fahrni, C. J., Culotta, V. C., Penner-Hahn, J. E., and O'Halloran, T. V. (1997) Metal ion chaperone function of the soluble Cu(I) receptor Atx1, *Science 278*, 853−6.

BI0511585